Magnetic properties of FePt nanodots formed by a self-assembled nanodot deposition method

doi: 10.1063/1.2335588

Magnetic properties of FePt nanodots formed by a self-assembled nanodot deposition method

C. K. Yin,[a] T. Fukushima, T. Tanaka, and M. Koyanagi
Department of Bioengineering and Robotics, Tohoku University, 6-6-01 Aza Aoba, Aramaki, Aoba-ku, Sendai 980-8579, Japan

J. C. Bea and H. Choi
Japan Science and Technology Agency (JST), 6-6-01 Aza Aoba, Aramaki, Aoba-ku, Sendai 980-8579, Japan

M. Nishijima
Institute for Materials Research, Tohoku University, 2-1-1 Katahira, Aoba-ku, Sendai 980-8577, Japan

M. Miyao
Department of Electronics, Kyushu University, 6-10-1 Hakozaki, Fukuoka 812-8581, Japan

(Received 3 May 2006; accepted 24 June 2006; published online 8 August 2006)

$Fe_{50}Pt_{50}$ nanodots dispersed in a SiO_2 film ($Fe_{50}Pt_{50}$ nanodot film) were formed by a self-assembled nanodot deposition (SAND) method in which $Fe_{50}Pt_{50}$ and SiO_2 are cosputtered in a high vacuum rf magnetron sputtering equipment. $Fe_{50}Pt_{50}$ pellets are laid on a SiO_2 target in a sputtering chamber to form the $Fe_{50}Pt_{50}$ nanodot film in the SAND method. The size and density of $Fe_{50}Pt_{50}$ nanodot were controlled by changing the ratio of the total area of $Fe_{50}Pt_{50}$ pellets to that of SiO_2 target. The $Fe_{50}Pt_{50}$ nanodot size decreases and its density increases when the ratio decreases. As-deposited $Fe_{50}Pt_{50}$ nanodots self-assembled to a face-centered-cubic phase of single-crystal structure. The $Fe_{50}Pt_{50}$ nanodot films were annealed to evaluate the nanodot size controllability, the magnetic anisotropy, and the thermal stability. Fully ordered $L1_0$ face-centered-tetragonal $Fe_{50}Pt_{50}$ nanodots with high magnetocrystalline anisotropy ($K_u \cong 8.7 \times 10^7$ ergs/cm^3) were obtained by *in situ* annealing at 600 °C for 1 h in a high vacuum ambience. Furthermore, the $Fe_{50}Pt_{50}$ nanodot film with a monolayer of $Fe_{50}Pt_{50}$ nanodots was formed by annealing at 800 °C due to the agglomeration of $Fe_{50}Pt_{50}$ nanodots in the SiO_2 film. © *2006 American Institute of Physics*.
[DOI: 10.1063/1.2335588]

FePt nanodot with $L1_0$ face-centered-tetragonal (fct) structure has attracted considerable attention owing to its potentials for new applications in the future including an ultrahigh density magnetic data storage and a novel nonvolatile memory which are produced by its high magnetocrystalline anisotropy. High density metal nanodots can be also employed in single electron devices. For such applications, it is necessary to develop a new formation method for ultrahigh density nanodot layer which enables to precisely control the nanodot size and density.[1–8] Recently, Sun *et al.* reported the magnetic recording properties of self-assembled FePt nanodots having a diameter of 3–10 nm which are synthesized by a chemical method.[1] For such FePt nanodots synthesized by a chemical method to give rise to ferromagnetic properties, it is required to convert the nanodot structure from a chemically disordered face-centered-cubic (fcc) phase to a chemically ordered fct phase. It is necessary to anneal FePt nanodots at a temperature higher than 600 °C for the phase conversion of FePt nanodots to a fully ordered $L1_0$ fct phase which provides the ferromagnetic properties. However, it is very difficult to control the nanodot size and density in chemically synthesized FePt nanodots after such high temperature annealing due to the agglomeration of FePt nanodots.[1–4]

In this study, a self-assembled nanodot deposition (SAND) method has been employed for the formation of FePt nanodots.[9,10] $Fe_{50}Pt_{50}$ nanodots dispersed in a SiO_2 film ($Fe_{50}Pt_{50}$ nanodot film) were formed on a silicon substrate with 10 nm thick SiO_2 on its surface at room temperature by the SAND method. The sputtering target material with different $Fe_{50}Pt_{50}$ compositions has been used for controlling the size and density of the $Fe_{50}Pt_{50}$ nanodots. The $Fe_{50}Pt_{50}$ composition was controlled by changing the number of $Fe_{50}Pt_{50}$ pellets having a length of 5 mm, a width of 5 mm, and a thickness of 1.5 mm which are laid on a SiO_2 target. The $Fe_{50}Pt_{50}$ nanodot films were deposited by using a high vacuum rf magnetron sputtering equipment. To obtain uniform dot size and dot density, the silicon substrate was rotated at a rate of 75 rpm/min. Figure 1 shows high resolution transmission electron microscopy (HRTEM) cross-sectional images of as-deposited $Fe_{50}Pt_{50}$ nanodot film produced with the $Fe_{50}Pt_{50}$ compositions of 8% and 12%. The $Fe_{50}Pt_{50}$ composition was defined as the ratio of total area of $Fe_{50}Pt_{50}$

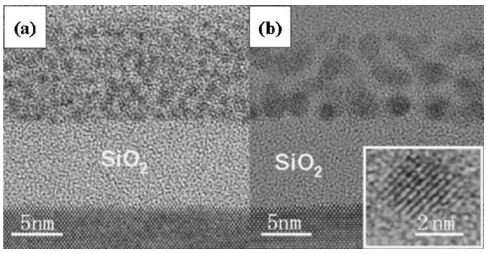

FIG. 1. HRTEM cross-sectional images of as-deposited $Fe_{50}Pt_{50}$ nanodot film (10 nm) formed on the silicon substrate with thermal SiO_2 (10 nm) on its surface. (a) $Fe_{50}Pt_{50}$ composition of 8%. (b) $Fe_{50}Pt_{50}$ composition of 12%.

[a]Electronic mail: yin@sd.mech.tohoku.ac.jp

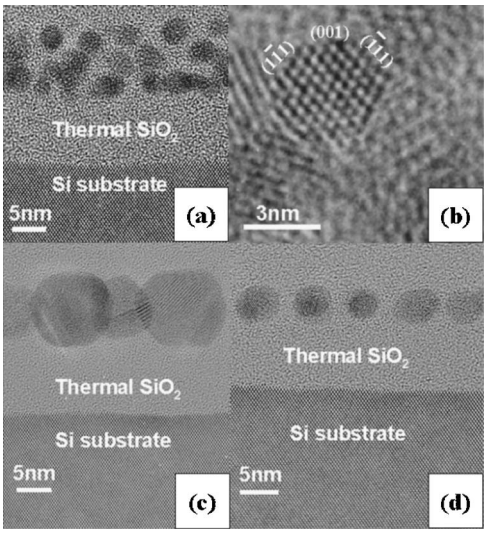

FIG. 2. HRTEM cross-sectional images of $Fe_{50}Pt_{50}$ nanodot films after annealing at various temperatures. The size of as-deposited $Fe_{50}Pt_{50}$ nanodots was 3.5–4.5 nm. (a) $Fe_{50}Pt_{50}$ nanodot film after annealing at 600 °C for 1 h. (b) An enlarged image of $Fe_{50}Pt_{50}$ nanodot after annealing at 600 °C for 1 h. (c) $Fe_{50}Pt_{50}$ nanodot film with a thickness of 10 nm after annealing at 800 °C for 1 h. (d) $Fe_{50}Pt_{50}$ nanodot film with a thickness of 6 nm after annealing at 800 °C for 1 h.

pellets to the SiO_2 target area. It is clearly observed in the figure that the $Fe_{50}Pt_{50}$ nanodots were dispersed with high density in the sputtered SiO_2 film. It is also clear from Fig. 1(b) that as-deposited $Fe_{50}Pt_{50}$ nanodots self-assemble to a face-centered-cubic phase of single-crystal structures. The sizes of $Fe_{50}Pt_{50}$ nanodots produced with the $Fe_{50}Pt_{50}$ compositions of 8% and 12% were 0.9–1.2 and 3.5–4.5 nm, respectively. Moreover, the density of $Fe_{50}Pt_{50}$ nanodots produced with the $Fe_{50}Pt_{50}$ compositions of 8% and 12% were $2.5\times10^{13}/cm^2$ and $8.5\times10^{12}/cm^2$, respectively. It was thus found that the nanodot size decreased and the nanodot density increased when decreasing the $Fe_{50}Pt_{50}$ composition in the target. This indicates that the dot size and density can be controlled well by the $Fe_{50}Pt_{50}$ composition in SiO_2 target. Similar results were obtained in the $W-SiO_2$ nanodot film and the $Co-SiO_2$ nanodot film.[9–11]

The $Fe_{50}Pt_{50}$ nanodot film was annealed to improve the crystal qualities and the magnetic properties. Annealing was performed in a high vacuum ambience (1×10^{-5} Pa) to prevent the oxidation of $Fe_{50}Pt_{50}$ nanodots. The 0.9–1.2 nm $Fe_{50}Pt_{50}$ nanodot films show superparamagnetic properties after annealing at 400–800 °C for 1 h. In this study, the 3.5–4.5 nm $Fe_{50}Pt_{50}$ nanodot films were annealed to evaluate the nanodot size controllability, the magnetic anisotropy, and the thermal stability. Figure 2 shows HRTEM cross-sectional images of $Fe_{50}Pt_{50}-SiO_2$ nanodot films after annealing at different temperatures. As shown clearly in Fig. 2(a), the size of $Fe_{50}Pt_{50}$ nanodots was 3.5–4.5 nm and the density of $Fe_{50}Pt_{50}$ nanodots was $8.5\times10^{12}/cm^2$ after annealing at 600 °C for 1 h. It seems that the $Fe_{50}Pt_{50}$ nanodots do not agglomerate by annealing at 600 °C for 1 h since the nanodot size of as-deposited nanodot film was 3.5–4.5 nm. It was also confirmed that the $Fe_{50}Pt_{50}$ nanodots formed by the SAND method are thermally more stable when compared to chemically synthesized nanodots. Furthermore, it was confirmed from Fig. 2(b) that the $Fe_{50}Pt_{50}$ nanodots after annealing at 600 °C for 1 h have a fully ordered $L1_0$ fct structure. HRTEM cross-sectional images of $Fe_{50}Pt_{50}-SiO_2$ nanodot films after annealing at 800 °C for 1 h are shown in Figs. 2(c) and 2(d). The thickness of as-deposited $Fe_{50}Pt_{50}-SiO_2$ nanodot film was 10 nm in Fig. 2(c) and 6 nm in Fig. 2(d). It is clear in Figs. 2(c) and 2(d) that a monolayer of FePt nanodots was produced by annealing at 800 °C due to the agglomeration of $Fe_{50}Pt_{50}$ nanodots. In addition, it was confirmed by an energy-dispersive x-ray spectroscopy that during the agglomeration of $Fe_{50}Pt_{50}$ nanodots they have not penetrated into the thermal SiO_2 which is formed underneath the $Fe_{50}Pt_{50}-SiO_2$ nanodot films. Consequently it was found that the nanodot size after annealing was defined by the thickness of the as-deposited film.

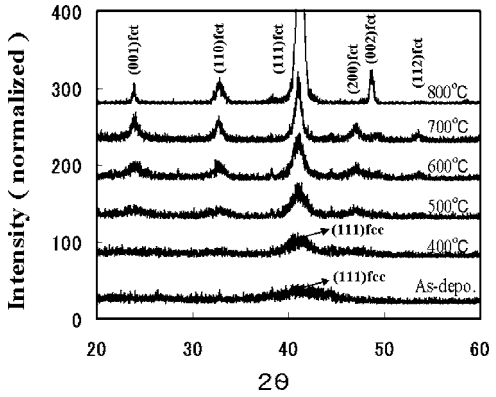

FIG. 3. XRD patterns of $Fe_{50}Pt_{50}$ nanodot films after annealing at various temperatures for 1 h.

Figure 3 shows x-ray diffraction (XRD) patterns of $Fe_{50}Pt_{50}$ nanodot film after annealing at various temperatures for 1 h. As-deposited nanodots exhibited the fcc structure with a broad peak which results from crystal defects in the nanodots. After annealing at 400 °C for 1 h, the fcc phase peak increased, indicating that the crystal defects decreased by thermal annealing. After 500 °C annealing, broad fct peaks of (111), (001), (100), (110), (200), and (112) appeared as the result of the phase transition. After annealing at a temperature of higher than 600 °C for 1 h, all of the fct peaks became clear, indicating that the nanodots converted into a fully ordered $L1_0$ phase. Furthermore, annealing at 700 and 800 °C caused the fct (111) peak to narrow and sharpen, indicating that the size of $Fe_{50}Pt_{50}$ nanodots increased by the agglomeration of $Fe_{50}Pt_{50}$ nanodots. These XRD results agree with HRTEM results.

Figure 4 shows the annealing temperature dependence of coercivity (H_c) which was measured by vibrating sample magnetometer (VSM). As is shown in the figure, the coerciv-

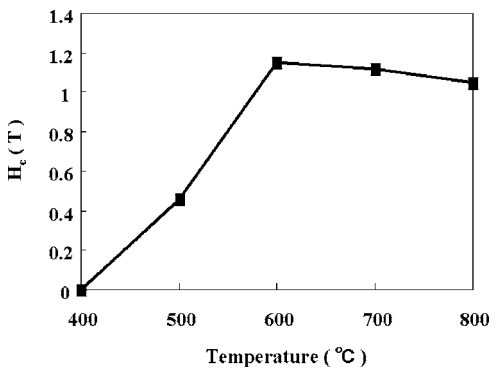

FIG. 4. Annealing temperature dependence of coercivity (H_c) in the $Fe_{50}Pt_{50}$ nanodot film which was measured by using VSM.

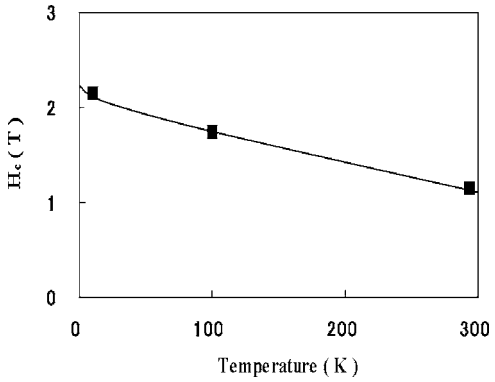

FIG. 5. Temperature dependence of coercivity (H_c) in the $Fe_{50}Pt_{50}$ nanodot film annealed at 600 °C for 1 h which was measured by using SQUID.

ity of 0.46 T was obtained after annealing at 500 °C for 1 h. In addition, we observed the maximum coercivity of 1.15 T after annealing at 600 °C, indicating that fully ordered $L1_0$ fct $Fe_{50}Pt_{50}$ nanodots were fabricated without agglomeration. Meanwhile the coercivity decreased to 1.12 and 1.05 T in the $Fe_{50}Pt_{50}$ nanodot films annealed at 700 and 800 °C for 1 h. It was considered that these decreases in coercivity resulted from the generation of polycrystalline phases in $Fe_{50}Pt_{50}$ nanodots. These VSM results also agree with XRD and HR-TEM results.

Figure 5 shows the temperature dependence of coercivity (H_c) in the $Fe_{50}Pt_{50}$ nanodot film annealed at 600 °C for 1 h which was measured by using a superconducting quantum interference device (SQUID). Such temperature dependence of coercivity (H_c) is described by the following equation:[5,6]

$$H_c = H_0\left(1 - \left(\frac{K_B T}{K_u V}\ln\left(\frac{t_m f_0}{\ln 2}\right)\right)^{2/3}\right), \quad (1)$$

where H_0 is the coercivity at 0 K, K_u is the magnetic anisotropy energy, V is the nanodot volume, K_B is the Boltzmann constant, t_m is the time for applying a magnetic field ($\sim$5 s), and f_0 is the thermal attempt frequency ($\sim 10^9$ Hz). By fitting the measured data to Eq. (1), we obtained the H_0 value of 2.15 T and the K_u value of approximately 8.7×10^7 ergs/cm^3. These values agree with those expected for fully ordered $L1_0$ FePt.

In conclusion, $Fe_{50}Pt_{50}$ nanodots dispersed in a SiO_2 film ($Fe_{50}Pt_{50}$ nanodot film) were formed by a SAND method. The $Fe_{50}Pt_{50}$ nanodot size decreased and the $Fe_{50}Pt_{50}$ nanodot density increased when decreasing the $Fe_{50}Pt_{50}$ composition of the target in the SAND method. The as-deposited $Fe_{50}Pt_{50}$ nanodots self-assembled to a fcc phase of single-crystal structures. Fully ordered $L1_0$ fct $Fe_{50}Pt_{50}$ nanodots with high magnetocrystalline anisotropy ($K_u \cong 8.7 \times 10^7$ ergs/cm^3) were produced by annealing at 600 °C for 1 h in a high vacuum ambience. In addition, the $Fe_{50}Pt_{50}$ nanodot film annealed at 600 °C exhibited the maximum coercivity of 1.15 T. Furthermore, a monolayer of $Fe_{50}Pt_{50}$ nanodots was produced by annealing at 800 °C due to the agglomeration of $Fe_{50}Pt_{50}$ nanodots. The $Fe_{50}Pt_{50}$ nanodot size in a monolayer could be defined by the $Fe_{50}Pt_{50}$ nanodot film thickness.

This work was performed in Venture Business Laboratory, Tohoku University, and supported by the Core Research for Evolutional Science and Technology (CREST) of Japan Science and Technology Agency (JST). The authors would like to thank S. Samukawa and S. Kono (both of Tohoku University) for their assistance and helpful discussions.

[1] S. H. Sun, C. B. Murray, D. Weller, L. Folks, and A. Moser, Science **287**, 1989 (2000).
[2] D. Weller, A. Moser, L. Folks, M. E. Best, W. Lee, M. F. Toney, M. Schwickert, J.-U. Thiele, and M. F. Doerner, IEEE Trans. Magn. **36**, 10 (2000).
[3] D. J. Sellmyer, C. P. Luo, M. L. Yan, and Y. Liu, IEEE Trans. Magn. **37**, 1286 (2001).
[4] H. Zeng, J. Li, J. P. Liu, Z. L. Wang, and S. H. Sun, Nature (London) **420**, 395 (2002).
[5] S. H. Sun, E. E. Fullerton, D. Weller, and C. B. Murray, IEEE Trans. Magn. **37**, 1239 (2001).
[6] Z. R. Dai, S. H. Sun, and Z. L. Wang, Nano Lett. **1**, 443 (2002).
[7] M. H. Lu, T. Song, T. J. Zhou, J. P. Wang, W. W. Ma, S. N. Piramanayagam, and H. Gong, J. Appl. Phys. **95**, 6735 (2004).
[8] B. Bian, D. Laoughlin, K. Sato, and Y. Hirotsu, J. Appl. Phys. **87**, 6962 (2000).
[9] M. Takada, S. Kondoh, T. Sakaguchi, H. Choi, J.-C. Shim, H. Kurino, and M. Koyanagi, Tech. Dig. - Int. Electron Devices Meet. **2003**, 553.
[10] T. Sakaguchi, Y. G. Hong, M. Kobayashi, H. Choi, J. C. Shim, H. Kurino, and M. Koyanagi Jpn. J. Appl. Phys., Part 1 **43**, 2203 (2004).
[11] C. K. Yin, J. C. Bea, Y. G. Hong, T. Fukushima, M. Miyao, K. Natori, and M. Koyanagi, Jpn. J. Appl. Phys., Part 1 **45**, 3217 (2006).